



Flange local buckling strength of hot-rolled steel W-shape solar array piers partially braced by soil

Cristopher D. Moen¹, Jake Morin², Andrew Thomsen³

Abstract

The local buckling strength of W-shaped hot-rolled steel pile piers braced by soil is approximated in this study. W-shaped piers are common foundations supporting solar arrays. For wind loadings, the piers experience flexural stresses below grade. The pier design and tight project economics typically call for some of the lightest W-sections available, and with corrosion section loss, the W-shape cross-sections are non-compact or slender at the end of their project design life. There is not much available information on how soil interaction with the pier underground might benefit local buckling strength. To explore this soil-structure interaction, finite strip elastic buckling analysis is used to approximate the critical elastic flange buckling stress of W-shaped piers in soil. The cross-section elastic buckling analysis includes linear springs that simulate the soil bracing on the cross-section, where the spring constant is related to common geotechnical parameters: soil subgrade modulus and the number of blows in a Standard Penetration Test. A parameter study is performed to calculate W-shape pier flange local buckling stress as a function of soil subgrade modulus, and this flange local buckling stress is used to calculate the local buckling strength with AISC 360-16. It is observed that the largest strength benefit from soil interaction occurs in the most locally slender W-shapes, although the maximum strength increase predicted was still less than 10 percent.

1. Introduction

Intuition tells us that when embedding locally slender steel members in soil, that the soil should provide partial restraint to local buckling deformation, and therefore some improvement in flexural or compressive ultimate strength. The challenge is to determine how much improvement, and this is the focus of the study summarized here, for hot-rolled steel pile piers.

The question of how soil influences local buckling is coming up frequently in the solar industry, where foundations for solar arrays are typically driven steel piles, see Fig. 1. A common design procedure is to consider pile pier corrosion section loss over the service life, which means that the piers becomes more and more locally slender with time. For the W6x7 cross-section considered

¹Owner, RunToSolve, LLC, <cris.moen@runtosolve.com>

²Principal, Structurology Inc. <jmorin@structurology.com>

³Senior Engineer, Structurology Inc. <athomsen@structurology.com>

in this study, the installed flange is 99.2 mm wide ($b_f = 3.905$ in.) and 4.06 mm thick ($t_f = 0.160$ in.), however nearing the end of its service life the flange is assumed to be 97.6 mm wide and 1.63 mm thick. With these reduced section dimensions, flange local buckling is in play as a strength limit state. The solar industry is in search of structural efficiency because of their high production volumes (driving millions of piles per year), and if there is an advantage to considering partial local bracing from soil in their foundations, the industry would benefit.



Figure 1: W-shape solar array piers

Research literature, design guidelines, and software cover foundation pier soil-structure interaction considering global (Euler) buckling and the soil subgrade modulus (units of pressure/length) (e.g., Reese and Wang 2006), however there is much less research available considering local buckling of thin-walled cross-sections embedded in soil. Local buckling of spirally welded thin-walled tubes in flexure filled with sand (Peters et al. 2015) showed that the sand did not prevent the initiation of local buckling deformation, but it did change the deformation field, preventing tube ovalization leading to higher post-buckling strengths when compared to tubes that were not filled with soil.

Classical plate buckling studies on an elastic foundation are useful for thinking through the potential benefits of soil bracing on local buckling. Critical elastic plate buckling stress solutions for an infinitely long simply-support plate on an elastic foundation are available (Seide 1958). In the range of soil foundation subgrade moduli ($5000 \text{ kN}/\text{m}^3$ for peat to $100000 \text{ kN}/\text{m}^3$ for clays to over $200000 \text{ kN}/\text{m}^3$ for gravelly sands and alluvium) and for the half-flange dimensions of the

corroded W6x7, the plate buckling stress increase is a maximum of 5 percent if the plate is fully attached, i.e., the plate pushes and pulls on the foundation. There is no increase in local buckling stress from soil bracing if the plate unattached, i.e., the plate pushes on the flexible foundation, but pulls off freely. These buckling stress changes from soil bracing are roughly determined using Seide (1958) Table 1 and Figure 2 where $\gamma \approx 0.15$ is defined on p. 382 and calculated with $\bar{k} = 200000\text{kN/m}^3$, $b=97.6\text{mm}/2$, $t=1.63$ mm. This calculation is not an apples-to-apples comparison because a W-shape pier flange has a free edge and Seide (1958) considers simply-supported plate boundary conditions, however the trends foreshadow the conclusions from this study.

Calculations are presented herein for the critical elastic flange local buckling stress of hot-rolled steel W-shaped piers (W6x7 and W6x25) driven into various soil types. It is assumed that the piers have experienced section loss from corrosion over a period of 40 years. The soil is modeled as distributed springs along the local buckling half-wave in finite strip eigenbuckling analyses performed with *CUFSM.jl*, a translation of CUFSM (Li and Schafer 2010) from MATLAB (MATLAB 2020) to the Julia language (Bezanson et al. 2017). Soil spring stiffness is approximated based on the number of blows N in a Standard Penetration Test (SPT). The pier local buckling flexural strength is also calculated using AISC 360-16 (AISC 2016) and recent W-shape local buckling research and commentary (Seif and Schafer 2010).

2. Pier Cross-Section Dimensions

The pier cross-sections considered in this study (gross section and corroded section) are the W6x7 (Fig. 2, Fig. 3) and the W6x25(Fig. 4, Fig. 5). The W6x7 corroded cross-section dimensions are $b_f=97.64\text{mm}$, $d=141.2\text{mm}$, $t_f=1.626\text{mm}$, and $t_w=0.864\text{mm}$. The W6x25 corroded cross-section dimensions are $b_f=152.0\text{mm}$, $d=157.2\text{mm}$, $t_f=9.119\text{mm}$, and $t_w=5.690\text{mm}$.

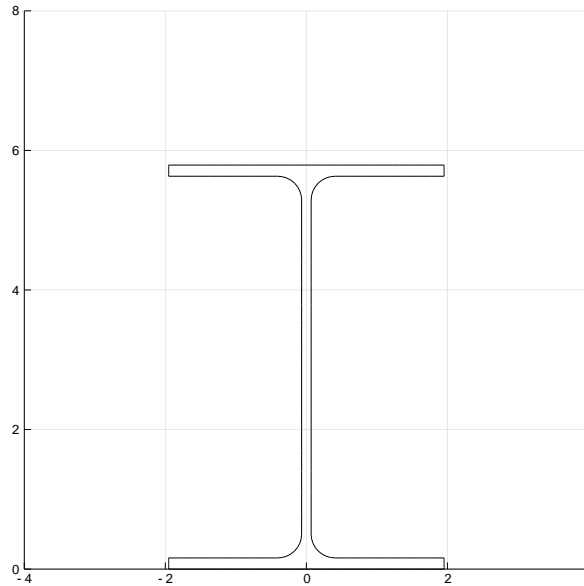


Figure 2: W6x7 gross cross-section

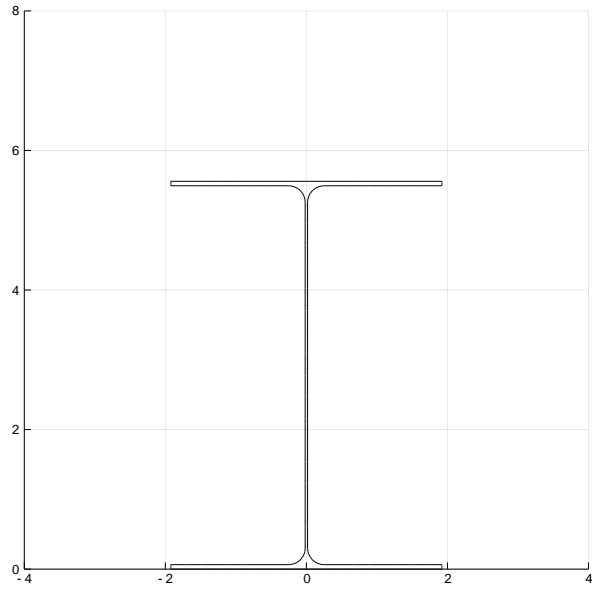


Figure 3: W6x7 corroded cross-section

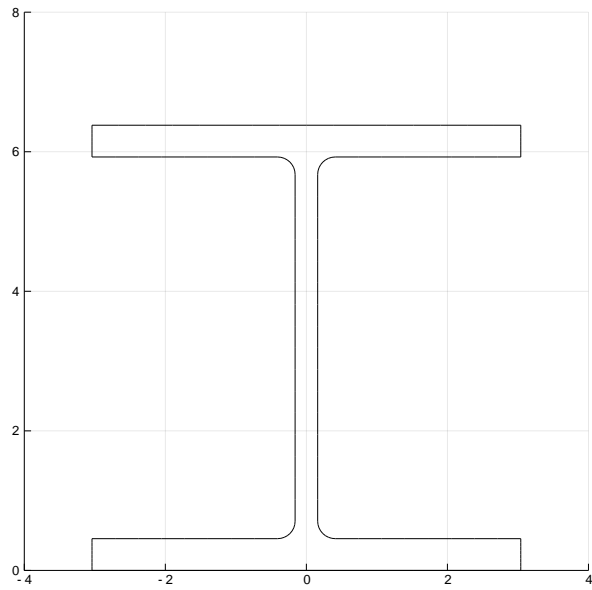


Figure 4: W6x25 gross cross-section

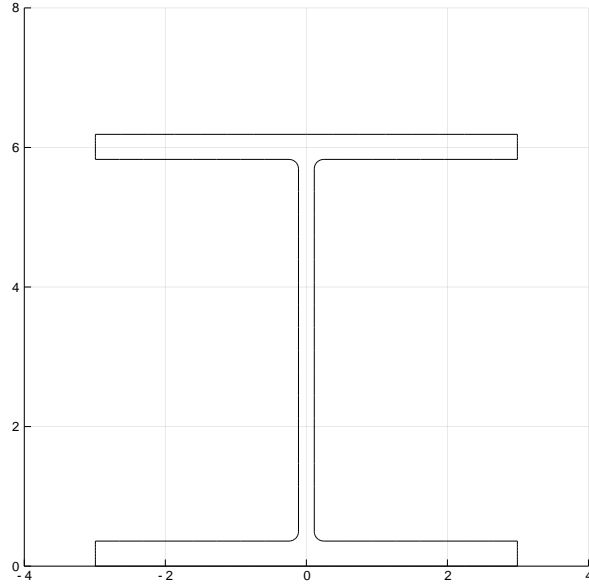


Figure 5: W6x25 corroded cross-section

3. Pier Local Buckling

The critical elastic flange local buckling strong axis flexural stress $F_{cr\ell}$ is calculated for each W-shape pier with CUFSM. The cross-sections are discretized as a centerline model, see Fig. 6 and Fig. 7. Transitions from web to flange in the W-shapes are not considered which is known to produce elastic buckling results typically within 5 percent of buckling loads calculated including the radii (Seif and Schafer 2010).

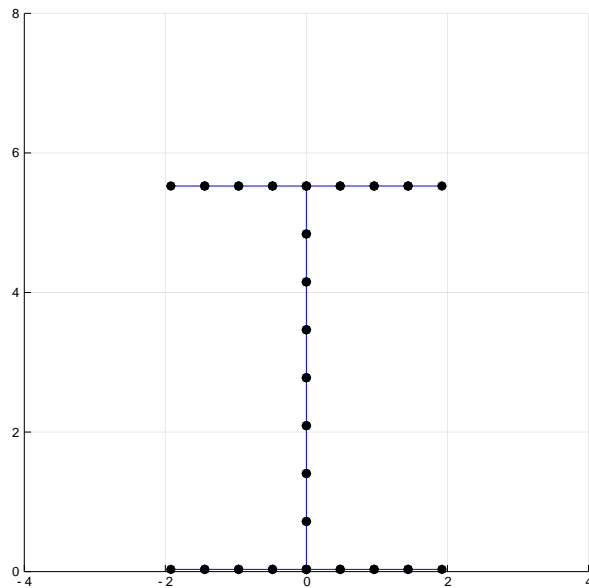


Figure 6: W6x7 corroded cross-section, discretized

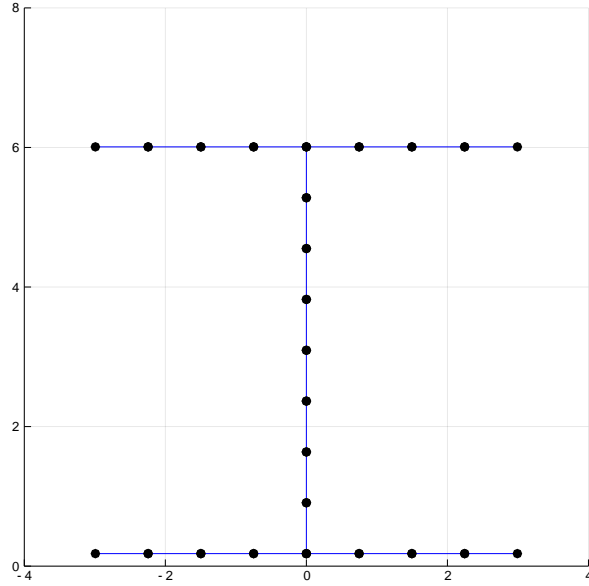


Figure 7: W6x25 corroded cross-section, discretized

The corroded W6x7 cross-section flange local buckling stress without considering partial soil restraint is $F_{cr\ell}=106.9$ MPa with a buckling half-wavelength $L_{cr\ell} = 214$ mm, see Fig. 8 for the mode shape. The corroded W6x25 cross-section flange local buckling stress without soil restraint is $F_{cr\ell}=1575$ MPa. The following sections will present an approach for considering partial soil restraint when calculating $F_{cr\ell}$.

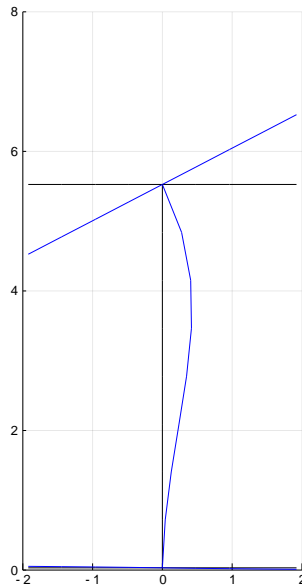


Figure 8: W6x7 corroded cross-section, flange local buckling

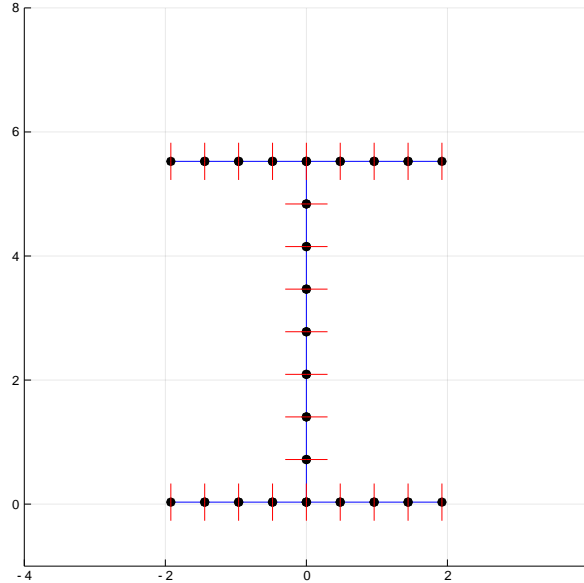


Figure 9: W6x7 with springs acting perpendicular to cross-section faces

4. Modeling Soil Stiffness

Partial bracing from soil can be included in a pier local buckling analysis by adding elastic distributed springs in CUFSM, where the springs act perpendicular to the pier cross-section faces at each cross-section node, see Fig. 9 showing the spring directions. In CUFSM, each node spring acts continuously along the pier which is reasonable for modeling soil, and the spring units are force/length/length. The springs are active in both directions. This is reasonable since if the flange buckles up or buckles down, it still reacts against soil. This is the 'attached' case in Seide(1958). Solar piles may also be driven into predrilled holes (not considered in this study), and this would be more like the 'unattached' case in Seide(1958) where the soil is only in contact with the outer faces of the pile cross-section.

A question yet to be answered though is how to calculate the CUFSM spring constant for soil, and specifically soil stiffness as a function of N from a Standard Penetration Test (SPT). For this study, a series of soil plate-load tests on consolidated clay (Rojas, Salinas, and Sejas 2007, Figure 3) were selected to guide a soil stiffness approximation. It was shown that the pressure-settlement relationship remains linear up to at least $0.40q_u$ where q_u is the ultimate strength of the soil.

What results from plate-load tests is often called a subgrade modulus, k_s , with units of $force/length^3$. In the Rojas et al.(2007) tests, the subgrade modulus in the linear range for unsaturated clay (test U5 for example) is $k_s = 200 \text{ kPa} / 0.0015 \text{ m} = 160000 \text{ kN}/\text{m}^3$. This subgrade modulus is very close in terms of units to the distributed spring constant input for CUFSM. If k_s is multiplied by the tributary width w for each node in the cross-section (i.e., group up all the subgrade modulus influence on one cross-section element and apply it at a node), then $k_{spring} = wk_s$ which has units of force/length/length which can be entered into the local buckling analysis.

One challenge with this approach is that plate-load field tests are not conducted for every pier installation. And so it would be convenient to relate k_{spring} generally to the number of blows N from a Standard Penetration Test. If one thinks of soil acting with the axial stiffness of a column of length L , then $k_{column} = E_s A / L$ where E_s is the soil elastic modulus and A is the soil column cross-sectional area. The column axial stiffness can also be written as a function of k_s because $k_s = P / A / \delta = k_{column} / A = E_s / L$, and reasonable values for E_s and L are all that are needed to approximate k_s for input into CUFSM.

There are widely debated empirical connections between the number of blows (N) in a Standard Penetration Test and soil elastic modulus. Bowles(1998) Table 5.5 provides such relationships, and a lower bound equation $E_s = 300(N + 6)$ (units of kPa) is used herein to cover a range of N values (0 to 60).

The Rojas et al.(2007) test results can be used to calculate a typical soil column length L . One can think of L as defining the region of soil influence a distance away from the faces of the pier cross-section. Assuming $N = 5$ and $k_s = 160000 \text{ kN/m}^2$ for consolidated clay, $E_s = 3300 \text{ MPa}$ with the empirical equation above, and then solving $k_s = E_s / L$ leads to $L = 21 \text{ mm}$. The soil column length L is small, which means that the soil region of influence is localized around the pier cross-section. This length L is assumed to remain constant when generalizing the calculation of $F_{cr\ell}$ in the next section.

5. W-Shape Pier Local Buckling in Soil

With a model for calculating the CUFSM soil spring as a function of the number of blows N in a Standard Penetration Test defined, it is possible to quantify the relationship between $F_{cr\ell}$ and N . For a range of N , E_s is calculated with the Bowles(1998) empirical equation, L is assumed as 21 mm defined previously, and CUFSM is used to calculate $F_{cr\ell}$ with springs arranged as in Fig. 9 and their magnitude $k_{spring} = w E_s / L$ where w is the node spacing in CUFSM.

For the corroded W6x7 cross-section, $F_{cr\ell} = 115.5 \text{ MPa}$ for $N = 60$ which is about 8 percent higher than $F_{cr\ell}$ without soil (106.9 MPa), see Fig. 10. For the corroded W6x25 cross-section, the soil bracing benefit is minimal, with $F_{cr\ell} = 1575.3 \text{ MPa}$ at $N = 60$ compared to $F_{cr\ell} = 1575.0 \text{ MPa}$ without soil influence, see Fig. 11. These results are consistent with the attached elastic foundation plate buckling trends from Seide(1958) described in the *Introduction* of this paper.

It is concluded that there is some small local buckling benefit from soil bracing for slender W-shape cross-sections, however in general, the bracing is not adequate to prevent the initiation of local buckling deformation. It is possible that the pier flanges might find local post-buckling stiffness and strength as the pier deforms and the soil compacts (see Peters et al. 2015 for an example of this, although these experiments are on tubes, not open cross-sections). Local post-buckling behavior of W-shaped piers in soil could be considered in a finite element study with soil and steel material and geometric nonlinearity.

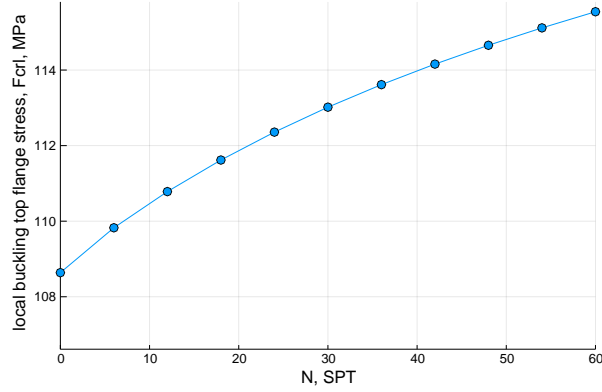


Figure 10: W6x7 flexural critical elastic flange local buckling stress as a function of the number of blows N from a Standard Penetration Test (SPT)

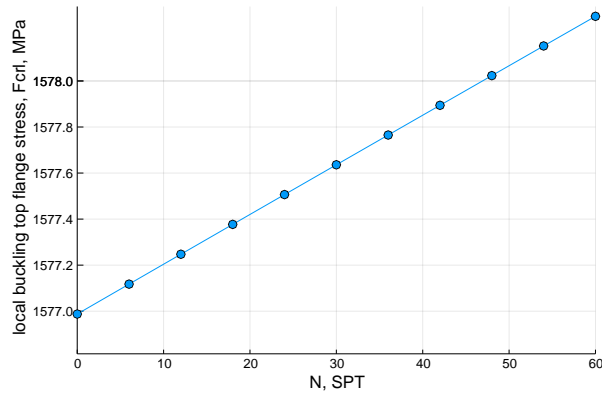


Figure 11: W6x25 flexural critical elastic flange local buckling stress as a function of the number of blows N from a Standard Penetration Test (SPT)

6. AISC 360-16 Pier Flexural Strength

The critical elastic flange buckling stress $F_{crℓ}$ approximated above can be used to calculate the nominal AISC flexural strength of the W-shaped piers. The procedure for defining AISC 360-16 Table B4.1 cross-section element slenderness limits is not fully known as discussed in Seif and Schafer (2010), however it is clear classical plate buckling equations are used. The AISC definition of $F_{crℓ} = [k\pi^2 E / (12(1 - \nu^2))] (t/b)^2$ where k is the plate buckling coefficient that depends on plate boundary conditions and b is the plate width. For the case of flange local buckling, typically $k = 0.43$ and assuming half of the flange is a plate, $b = b_f/2$. The plate edge at the web is assumed simply-supported, and the plate edge at the tip of the compressed flange is free.

A general form of cross-sectional slenderness is $\alpha = \sqrt{F_y / F_{crℓ}}$ which is helpful in this soil study because $F_{crℓ}$ is calculated including the influence of soil. Seif and Schafer (2010) derive an equation that relates α to k and the AISC cross-section slenderness limit $b/t = \beta \sqrt{E / F_y}$ which is $\alpha = \sqrt{12\beta^2(1-\nu^2) / (k\pi^2)}$. This useful transformation allows the equivalent AISC b/t limits for slenderness to be calculated in terms of α .

In AISC 360-16 Table B4.1b, Case 10, $\beta_p = 0.38$ which leads to $\alpha_p = 0.61$, the compact to non-compact transition limit, using the Seif and Schafer (2010) equation described above, with $k = 0.43$. Similarly, in AISC 360-16 Table B4.1b, Case 10, $\beta_r = 1.0$ which leads to $\alpha_r = 1.60$, the non-compact to locally slender transition limit.

For the corroded W6x7 cross-section driven in soil with $N=60$, $\alpha = \sqrt{345\text{MPa}/115.5\text{MPa}}=1.72$ which is greater than α_r , and therefore the cross-section is locally slender and AISC 360-16 Eq. F3-2, $M_n = 0.9Ek_cS_x/\lambda^2$, should be used. The flange plate buckling coefficient $k_c=0.58$ can be calculated from $F_{cr\ell} = [k\pi^2E/(12(1-\nu^2))](t/b)^2$ using $F_{cr\ell}=115.5\text{MPa}$, $S_x = 24744\text{mm}^3$ for the corroded cross-section, and AISC 360-16 Eq. F3.2 where $\lambda = b_f/(2t_f)=30.0$. Using all of these values leads to $M_n=2835\text{ kN-mm}$ which is the predicted flange local buckling flexural strength considering the influence of soil. If soil is not considered, then $k_c=0.53$ (using $F_{cr\ell}=106.9\text{MPa}$) and $M_n=2590\text{ kN-mm}$. And if the AISC 360-16 equation $k_c = 4/\sqrt{h/t_w}$ is used, then $k_c=0.35$ and $M_n=1710\text{ kN-mm}$.

7. Conclusions

Soil has a small beneficial influence on pier flange local buckling. Soil is not stiff enough to brace against the initiation of local buckling deformation for the W-shaped piers considered, however there may be local post-buckling deformation restraint possible, and this was not considered. The benefits are highest for the most locally slender corroded W6x7 cross-section where there is an 8 percent increase in flange local buckling stress when the pier is driven into a stiff soil with a Standard Penetration Test blow count of 60.

References

- AISC (2016). *Specification for Structural Steel Buildings, ANSI/AISC 360-16*. American Institute of Steel Construction.
- Bezanson, Jeff et al. (2017). “Julia: A fresh approach to numerical computing”. *SIAM review* 59.1, pp. 65–98. URL: <https://doi.org/10.1137/141000671>.
- Bowles, J.E. (1998). *Foundation Analysis and Design*. 6th. McGraw-Hill International Press.
- Li, Z and Benjamin W Schafer (2010). “Buckling analysis of cold-formed steel members with general boundary conditions using CUFSM conventional and constrained finite strip methods”. *20th International Specialty Conference on Cold-Formed Steel Structures*. St. Louis, MO.
- MATLAB (2020). *version 9.9.0 (R2020b)*. Natick, Massachusetts: The MathWorks Inc.
- Peters, Dirk Jan et al. (2015). “Local buckling resistance of sand-filled spirally welded tubes”. *The Twenty-fifth International Ocean and Polar Engineering Conference*. OnePetro.
- Reese, Lymon C and Shin-Tower Wang (2006). “Verification of computer program LPile as a valid tool for design of a single pile under lateral loading”. URL: https://ensoftinc.com/main/products/pdf/Lpile-Validation_Notes.pdf.
- Rojas, Juan Carlos, Luis Mauricio Salinas, and Claudia Sejas (2007). “Plate-load tests on an unsaturated lean clay”. *Experimental unsaturated soil mechanics*. Springer, pp. 445–452.
- Seide, Paul (1958). “Compressive buckling of a long simply supported plate on an elastic foundation”. *Journal of the Aerospace Sciences* 25.6, pp. 382–384.
- Seif, Mina and Benjamin W Schafer (2010). “Local buckling of structural steel shapes”. *Journal of Constructional Steel Research* 66.10, pp. 1232–1247.